

# Optical Engineering

OpticalEngineering.SPIEDigitalLibrary.org

## **Simulation and experimental research on the Alamouti code for ultraviolet communication**

Li Guo  
Kunlun Liu  
Dedan Meng  
Xidong Mu  
Dahai Han

# Simulation and experimental research on the Alamouti code for ultraviolet communication

Li Guo,<sup>a,\*</sup> Kunlun Liu,<sup>a</sup> Dedan Meng,<sup>a</sup> Xidong Mu,<sup>a</sup> and Dahai Han<sup>b</sup>

<sup>a</sup>Beijing University of Posts and Telecommunications, Key Lab of Universal Wireless Communications, Ministry of Education, No. 10 Xitucheng Road, Beijing 100876, China

<sup>b</sup>Institute of Information Photonics and Optical Communications, No. 10 Xitucheng Road, Beijing 100876, China

**Abstract.** The Alamouti code can obtain the diversity gain utilizing the transmitting signal orthogonally without the use of a complicated decoding scheme. The modified Alamouti code for the ultraviolet (UV) communication system is studied in theoretical analysis, MATLAB<sup>®</sup> simulation, and offline experiment. The theoretical analysis and simulation results indicate that the usage of the Alamouti code in the UV communication system can achieve a higher diversity gain and reduce the system bit error rate more effectively than the single-input single-output and single-input multiple-output technologies. The experiments were performed to verify the simulation results. Next, we analyzed the discrepancy between the simulation results and the experimental results. These studies are helpful for UV multiple-input multiple-output communication system design and implementation. © The Authors. Published by SPIE under a Creative Commons Attribution 3.0 Unported License. Distribution or reproduction of this work in whole or in part requires full attribution of the original publication, including its DOI. [DOI: [10.1117/1.OE.55.1.015101](https://doi.org/10.1117/1.OE.55.1.015101)]

Keywords: multiple-input multiple-output; Space Time Code; Alamouti; ultraviolet communication.

Paper 151092 received Aug. 10, 2015; accepted for publication Nov. 23, 2015; published online Jan. 4, 2016.

## 1 Introduction

Multiple-input multiple-output (MIMO) technology<sup>1</sup> spatially extends the communication resources and achieves spatial diversity and multiplexing using multiple input and multiple output antenna technology. It yields a larger channel capacity and better transmission reliability.<sup>2,3</sup>

The Space Time Code (STC) is the typical representative of MIMO technology. STC encodes the original transmitting sequences into redundant sequences using a two-dimensional interval and spatial encoding method. The encoded signals are transmitted in parallel using the multiple transmitting antennas.<sup>4</sup>

The Alamouti<sup>5</sup> code is one of the simplest and useful STC methods that is suitable for two transmitting antennas. The code obtains the diversity gain via the orthogonality between the different transmitting antennas and linear convergence of the different receiving antennas.

Ultraviolet (UV) communication is an emerging and safe communication method whereby data are transmitted by using the scattering of UV light in the atmosphere with its capabilities of nonline-of-sight (NLOS) communication, anti-interception, and anti-interference. However, UV communication has disadvantages, such as multipath fading and intersymbol interference.<sup>6</sup>

Few studies have been performed to enhance the UV system using MIMO technology. MIMO technology was studied for infrared<sup>7</sup> and for lasers in atmospheric channels with coherent detection<sup>8</sup> and pulse-position modulation (PPM).<sup>9</sup> A series of research identified the types of space-time coding in the UV system,<sup>10,11</sup> and the receiver of UV MIMO system was designed theoretically,<sup>12</sup> but they did not involve any real environment experiments.

In this paper, the modified Alamouti code is adopted in the UV communication system to obtain the diversity gain

by utilizing the orthogonality of the transmitting signals. The simulation results and offline experimental results indicate that the Alamouti code can reduce the system bit error rate (BER) more effectively than the single-input single-output (SISO) and single-input multiple-output (SIMO) technologies.

The paper is organized as follows. Following the introduction in Sec. 1, the system model of NLOS UV MIMO communication system with modified Alamouti encoding and decoding is presented in Sec. 2. The simulation schematics and results are described in Sec. 3. Section 4 describes the system offline experiments. Section 5 analyzes the difference between the simulation results and the experimental results. The conclusion of the paper is provided in Sec. 6.

Throughout the paper,  $\{\cdot\}$  denotes a set, vectors are denoted by boldface lowercase letters, and matrices are denoted by boldface uppercase letters.

## 2 System Model of Nonline-of-Sight Ultraviolet Multiple-Input Multiple-Output Communication with Modified Alamouti Code

### 2.1 System Model

In the UV communication system, the transmitted signal has intensity modulations, such as ON-OFF keying (OOK) and PPM, because the negative signal cannot be detected at the receiver, such as that in the free-space optical systems.<sup>13</sup> In this paper, a modified Alamouti code that Simon and Vilmrotter proposed<sup>14</sup> with OOK modulation is adopted in the UV communication system. The schematic diagram of the  $2 \times 2$  UV MIMO communication system is illustrated in Fig. 1. The system consists of three parts. The first part is the transmitters, where two UV light-emitting diodes (LEDs) are modulated to carry the data with the modified Alamouti encoding. The propagation channel is an NLOS UV communication link, through which the UV light becomes scattered. The third part is the receivers, where

\*Address all correspondence to: Li Guo, E-mail: [guoli@bupt.edu.cn](mailto:guoli@bupt.edu.cn)

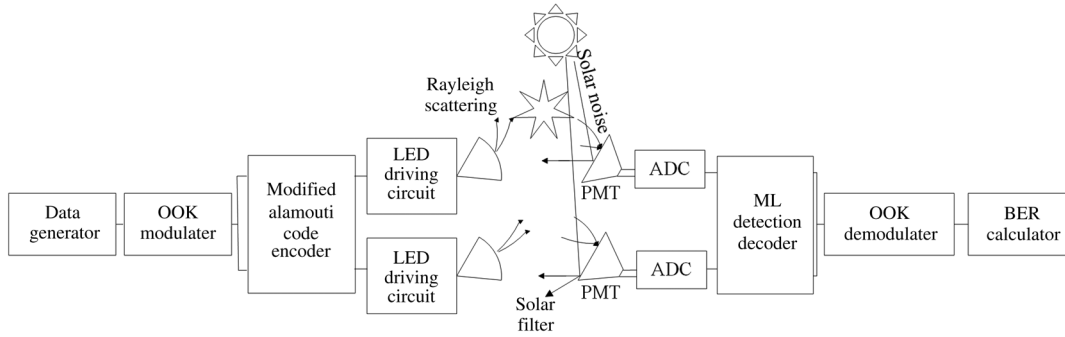


**Fig. 1** Nonline-of-sight (NLOS) ultraviolet (UV) multiple-input multiple-output communication system schematic diagram.

two photomultiplier tubes (PMTs) are used for light detection before the modified Alamouti decoding.

The geometrical diagram of the  $2 \times 2$  MIMO UV communication system is shown in Fig. 2. The transmitter (Tx) beam full-width divergence angle is denoted by  $\varphi_1$ , the receiver (Rx) field-of-view angle is denoted by  $\varphi_2$ , the Tx elevation angle is denoted by  $\theta_1$ , Rx elevation angle is denoted by  $\theta_2$ , and the Tx and Rx baseline distance is denoted by  $r$ . Both the distances between the two Tx antennas and that between the two PMTs are  $d$ .

## 2.2 Modified Alamouti Code in NonLine-of-Sight Ultraviolet Multiple-Input Multiple-Output Communication System

In the conventional Alamouti code,  $x_1, x_2$  are transmitted from Tx1 and Tx2, respectively, in the first bit interval, and  $-x_2, x_1$  are transmitted from Tx1 and Tx2, respectively, in the second bit interval. All of the transmitted signals are real number signals in the UV communication system, so the modified Alamouti code<sup>14</sup> is used in the NLOS UV communication system.

Assume that two signals  $x_1$  and  $x_2$  are sent at Tx1 and Tx2, respectively, in the  $2 \times 2$  UV system, and  $x_1, x_2$  each ranges over the signal set  $\{0, A\}$ , where  $A$  is the amplitude of the transmitted signal related to the intensity of the light source. The modified code matrix<sup>14</sup> is denoted by

$$\mathbf{X} = \begin{bmatrix} x_1 & A - x_2 \\ x_2 & x_1 \end{bmatrix}. \quad (1)$$

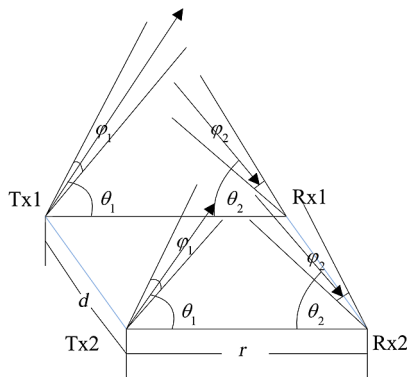


**Fig. 2** NLOS UV communication link geometry, depicting elevated beam full-width divergence and field of view.

The first column of  $\mathbf{X}$  denotes the transmitted signals from the two antennas, in the first bit interval, and the second column denotes the transmitted signals from two antennas in the second bit interval. From the matrix, we recognize that the transmitted signal is always non-negative. The channel gain matrix is denoted by

$$\mathbf{H}(\theta_1, \theta_2, \varphi_1, \varphi_2, r, d) = \begin{bmatrix} h_{11}(\theta_1, \theta_2, \varphi_1, \varphi_2, r_{11}, d) & h_{12}(\theta_1, \theta_2, \varphi_1, \varphi_2, r_{12}, d) \\ h_{21}(\theta_1, \theta_2, \varphi_1, \varphi_2, r_{21}, d) & h_{22}(\theta_1, \theta_2, \varphi_1, \varphi_2, r_{22}, d) \end{bmatrix}. \quad (2)$$

A Monte Carlo model<sup>15</sup> is adopted as the NLOS UV scattering channel.  $h_{ji}(\theta_1, \theta_2, \varphi_1, \varphi_2, r_{ji}, d)$  is the channel gain from the  $i$ 'th transmitting antenna to the  $j$ 'th receiving PMT, and  $r_{ji}$  is the distance between the  $i$ 'th transmitting antenna and the  $j$ 'th receiving PMT, where  $i, j \in \{1, 2\}$ ; the elements  $h_{ji}(\theta_1, \theta_2, \varphi_1, \varphi_2, r_{ji}, d)$  of  $\mathbf{H}(\theta_1, \theta_2, \varphi_1, \varphi_2, r, d)$  are real numbers, which are only related to  $\theta_1, \theta_2, \varphi_1, \varphi_2, r$ , and  $d$ .

The received signals of the  $l$ 'th PMT in the first bit interval  $y_{l1}$  and the second bit interval  $y_{l2}$ ,  $l = 1, 2$ , are given by

$$\begin{aligned} y_{l1} &= x_1 h_{l1}(\theta_1, \theta_2, \varphi_1, \varphi_2, r_{l1}, d) \\ &\quad + x_2 h_{l2}(\theta_1, \theta_2, \varphi_1, \varphi_2, r_{l2}, d) + n_{l1}, \\ y_{l2} &= (A - x_2) h_{l1}(\theta_1, \theta_2, \varphi_1, \varphi_2, r_{l1}, d) \\ &\quad + x_1 h_{l2}(\theta_1, \theta_2, \varphi_1, \varphi_2, r_{l2}, d) + n_{l2}, \end{aligned} \quad (3)$$

where  $n_{l1}$  and  $n_{l2}$  are independent receiving noises in the two receivers, which consist of sunlight noise, PMT dark current noise, and receiver transimpedance amplifier (TIA) output noise.

The analog-to-digital converter converts the analog signal  $y_{li}l$ ,  $i = 1, 2$  to the corresponding digital signal; the digital signal is then processed through the integrate-and-dump filter, which is a matched filter used for maximizing the signal-to-noise ratio (SNR) in the presence of additive stochastic noise.

Assuming the channel gain and the amplitude of the transmitted signal are pre-known by the receivers, the receivers can use  $y_{l1}, y_{l2}$  signals to reconstruct the transmitted signals  $x_1, x_2$  as  $\tilde{x}_1, \tilde{x}_2$ , where  $\tilde{x}_1, \tilde{x}_2$  are denoted by the following formulas:

$$\begin{aligned}
 \tilde{x}_1 &= \sum_{l=1}^{L=2} y_{l1} h_{l1}(\theta_1, \theta_2, \varphi_1, \varphi_2, r_{l1}, d) \\
 &+ \sum_{l=1}^{L=2} y_{l2} h_{l2}(\theta_1, \theta_2, \varphi_1, \varphi_2, r_{l2}, d) \\
 &- A \sum_{l=1}^{L=2} h_{l1}(\theta_1, \theta_2, \varphi_1, \varphi_2, r_{l1}, d) h_{l2}(\theta_1, \theta_2, \varphi_1, \varphi_2, r_{l2}, d), \\
 \tilde{x}_2 &= \sum_{l=1}^{L=2} y_{l1} h_{l2}(\theta_1, \theta_2, \varphi_1, \varphi_2, r_{l2}, d) \\
 &- \sum_{l=1}^{L=2} y_{l2} h_{l1}(\theta_1, \theta_2, \varphi_1, \varphi_2, r_{l1}, d) \\
 &+ A \sum_{l=1}^{L=2} h_{l1}^2(\theta_1, \theta_2, \varphi_1, \varphi_2, r_{l1}, d). \tag{4}
 \end{aligned}$$

Substituting Eq. (3) into Eq. (4), we obtain the following simplified results:

$$\begin{aligned}
 \tilde{x}_1 &= x_1 \sum_{l=1}^{L=2} [h_{l1}^2(\theta_1, \theta_2, \varphi_1, \varphi_2, r_{l1}, d) + h_{l2}^2(\theta_1, \theta_2, \varphi_1, \varphi_2, r_{l2}, d)] \\
 &+ \sum_{l=1}^{L=2} [n_{l1} h_{l1}(\theta_1, \theta_2, \varphi_1, \varphi_2, r_{l1}, d) \\
 &+ n_{l2} h_{l2}(\theta_1, \theta_2, \varphi_1, \varphi_2, r_{l2}, d)], \\
 \tilde{x}_2 &= x_2 \sum_{l=1}^{L=2} [h_{l1}^2(\theta_1, \theta_2, \varphi_1, \varphi_2, r_{l1}, d) + h_{l2}^2(\theta_1, \theta_2, \varphi_1, \varphi_2, r_{l2}, d)] \\
 &+ \sum_{l=1}^{L=2} [n_{l1} h_{l2}(\theta_1, \theta_2, \varphi_1, \varphi_2, r_{l2}, d) \\
 &- n_{l2} h_{l1}(\theta_1, \theta_2, \varphi_1, \varphi_2, r_{l1}, d)]. \tag{5}
 \end{aligned}$$

From Eq. (5), we can see the interference between two Tx antennas is eliminated due to the contribution of the modified Alamouti code.

The maximum likelihood (ML) decision rule is used, which requires both the received signals and the transmitted signal set. As the pair of transmitted signals is independently chosen from the signal set, the best decision made separately on each of them is given by

$$\begin{aligned}
 \hat{x}_i &= \underset{x_i}{\operatorname{argmin}} \left( (\tilde{x}_i - x_i)^2 + \left\{ \sum_{l=1}^{L=2} [h_{l1}^2(\theta_1, \theta_2, \varphi_1, \varphi_2, r_{l1}, d) \right. \right. \\
 &\left. \left. + h_{l2}^2(\theta_1, \theta_2, \varphi_1, \varphi_2, r_{l2}, d)] - 1 \right\} x_i^2 \right), \tag{6}
 \end{aligned}$$

where  $x_i$ ,  $i = 1, 2$  ranges over the signal set  $\{0, A\}$ . From Eq. (6), the ML decision method strongly depends on the channel state information (CSI). Thus, the performance of the modified Alamouti code in UV communication is determined by how perfect the channel state information obtained by the receivers is.

### 3 Simulation and Results

The simulations were based on the MATLAB<sup>®</sup> platform. Pseudo-noise (PN) sequences were OOK modulated and encoded as the modified Alamouti code. The NLOS UV single-scatter model is too simple and easily neglected, so multiple-scattering model is adopted. The scattering of photon is random and multiple-scattering process is a succession of elementary events whose probability laws are known.<sup>16</sup> To depict the photon multiple-scattering phenomenon, the Monte Carlo method is adopted to obtain the UV communication system channel fading factors. The PMT amplification factor was  $6.3 \times 10^5$  and the PMT cathode radiant sensitivity (265 nm) was 62 mA/W. The sunlight noise and the TIA output noise were set, obeying the normal distribution. The PMT dark current noise was set fixed. The simulation parameters are listed in Column 1 of Table 1.

In the first simulation, we considered the system BER performance with respect to the distance between Tx and Rx. The Tx and Rx elevation angles were both fixed at 10 deg. The distances between the two LEDs and the two PMTs were both set at 2 m. The distance between the Tx and the Rx ranged from 8 to 30 m. The BERs of the UV system using SISO,  $1 \times 2$  maximal ratio combining (MRC),  $2 \times 1$  Alamouti code, and  $2 \times 2$  Alamouti code were compared. The simulation result is shown in Fig. 3. The modified Alamouti code exhibits better performance in the UV communication system. The diversity gain of the  $2 \times 1$  Alamouti code scheme has better performance compared with that of the SISO. According to Ref. 5, the  $2 \times 1$  Alamouti code transmission system has the same diversity gain as the  $1 \times 2$  receiving diversity system. In Fig. 3, the performances of the  $1 \times 2$  MRC and the  $2 \times 1$  Alamouti code systems are almost the same because the channel difference between  $h_{l2}(\theta_1, \theta_2, \varphi_1, \varphi_2, r_{l2}, d)$  and  $h_{21}(\theta_1, \theta_2, \varphi_1, \varphi_2, r_{21}, d)$  is so small. The diversity gain of the  $2 \times 2$  Alamouti code scheme is twice of that in the  $2 \times 1$  Alamouti code scheme, as found from the slope of the two respective curves. When the distance increased, the number of received photons decreased, thus leading to the decrease of SNR. In Fig. 3, the BER of  $2 \times 2$  Alamouti is  $\sim 10^{-1.4}$  and the BER of SISO is  $\sim 10^{-0.9}$  when distance is 25 m. The simulation shows the modified Alamouti code can have both transmitting diversity gain and receiving diversity gain, and it works well in an NLOS UV communication system.

In the second simulation, the Tx elevation angle was fixed at 10 deg, the distance between the Tx and the Rx was 15 m, and the Rx elevation angle ranged from 0 to 27 deg. We can see from the results in Fig. 4 that the performance becomes worse with the increase of the Rx elevation angle. When the Rx elevation angle increased, the decreased number of received photons leads to the decrease of SNR. In Fig. 4, the BER of  $2 \times 2$  Alamouti is  $\sim 10^{-1}$  and the BER of SISO is  $\sim 10^{-0.82}$  when Rx elevation angle is 24 deg. In the third simulation, the Rx elevation angle was fixed at 10 deg, the distance between Tx and Rx was 15 m, and the Tx elevation angle ranged from 0 to 27 deg. The simulation result in Fig. 5 shows that when the Tx elevation angle increases, the BER becomes higher. The increased Tx elevation angle also leads to the decrease of SNR. In Fig. 5, the BER of  $2 \times 2$  Alamouti is  $10^{-0.8}$  and the BER of SISO is  $\sim 10^{-0.7}$  when Tx elevation angle is 24 deg. As the path loss is relevant to the Tx and Rx elevation

**Table 1** Comparison between the simulation and the experiment parameters.

Parameters	Column 1	Column 2
Number of PMTs	2	2
Power of UV source	1 mW	0.3 mW
Tx BFWD angle	17 deg	120 deg
Rx FOV angle	15 deg	30 deg
Distance between two PMTs	2 m	0.2 m
Distance between two UV LEDs	2 m	0.2 m
Transmitter elevation angle	0 to 27 deg, in 3 deg steps	0 to 27 deg, in 3 deg steps
Receiver elevation angle	0 to 27 deg, in 3 deg steps	0 to 27 deg, in 3 deg steps
Distance between the transmitters and the receivers	8 to 30 m, in 2 m steps	3 to 10.8 m, in 0.6 m steps
UV wavelength	265 nm	265 nm
Solar filter transmittance	0.2	0.2
Data rate of transfer	100 kbps	125 kbps
Sampling rate of ADC	8 MHz	2.5 MHz
Number of samples	80	20

Note: PMT, photomultiplier tube; UV, ultraviolet; Tx, transmitter; BFWD, beam full-width divergence; Rx, receiver; FOV, field of view; LED, light-emitting diode; ADC, analog-to-digital converter.

angles,<sup>17</sup> the performance is found to decrease with the increase of either the Tx elevation angle or the Rx elevation angle.

Although the fading in UV channel became worse because the distance and Rx elevation angle increased, respectively, MIMO still performed the best. As the distance and Rx elevation angle increase, especially >25 m and 24 deg, respectively, the SNR is too low with current transmitting power and the advantage of MIMO is not so obvious. So the four curves of Figs. 3 and 4 became close to each other, respectively.

### 4 System Experiment

Offline experiments based on a solar blind UV test-bed at the wavelength of 265 nm were performed. At the transmitter,

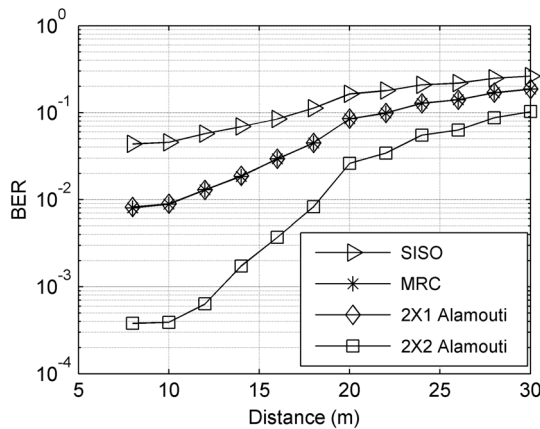


**Fig. 3** Bit error rate (BER) with respect to distance, using single-input single-output (SISO),  $1 \times 2$  maximal ratio combining (MRC), the  $2 \times 1$  Alamouti code scheme, and the  $2 \times 2$  modified Alamouti code scheme when the transmitter (Tx) and receiver (Rx) elevation angles are 10 deg.

a series of PN sequences were generated and encoded as the modified Alamouti code. Next, the encoded sequences were read by the signal generator to transmit.

At the receiver, two PMTs were set to receive the UV signal. The received UV light was changed to electronic signals by PMTs and the BER of the algorithm was calculated.

The experiment was performed on January 27, 2015, indoors. The detail of the experiment is shown in Fig. 6. The parameters of the experiment are presented in Column 2 of Table 1.

From Sec. 2, we know that the CSI is necessary in Alamouti scheme. So the CSI must be measured before the data transmission. In radio frequency communications, one ordinary way to get the CSI is to send sinusoidal

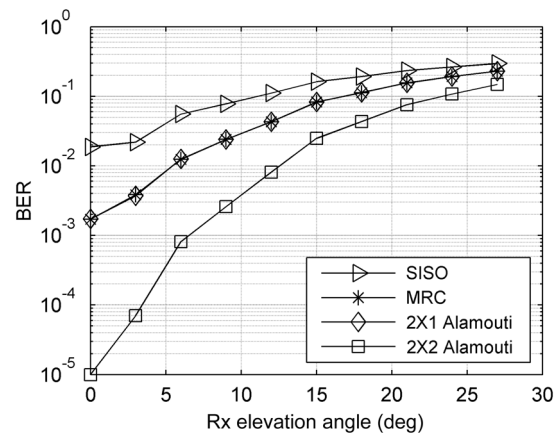


**Fig. 4** BER with respect to Rx elevation angle using SISO,  $1 \times 2$  MRC, the  $2 \times 1$  Alamouti code scheme, and the  $2 \times 2$  modified Alamouti code scheme when the Tx elevation angle is 10 deg.

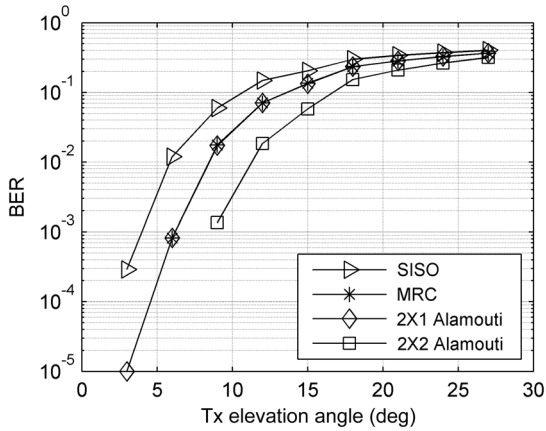


**Fig. 5** BER with respect to Tx elevation angle using SISO, 1 × 2 MRC, the 2 × 1 Alamouti code scheme, and the 2 × 2 modified Alamouti code scheme when the Rx elevation angle is 10 deg.

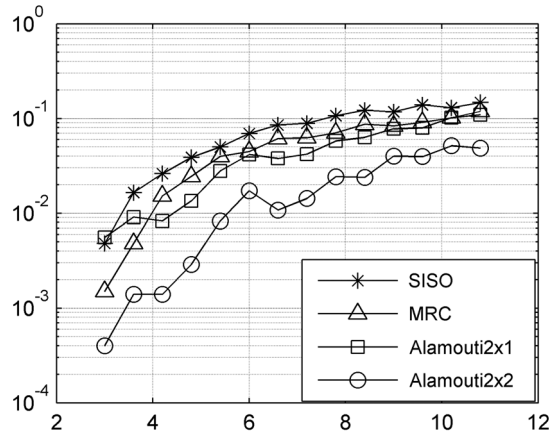


**Fig. 7** BER performance of four algorithms versus distance with Tx elevation of 10 deg and Rx elevation 0.

waves and calculate the CSI using the amplitude and phase of the received signal.<sup>18</sup> Based on this method, the CSI measurement in our system follows the steps below.

First, LED1 sends a series of data “1,” and the two receivers receive signals separately. These received signals are used to determine the channel gain from transmitter 1. Next, LED2 sends a series of data “1” alone, and the two receivers receive the signals separately, which is used to obtain the UV channel gain from this transmitter. After the procedure above,  $h_{ji}(\theta_1, \theta_2, \varphi_1, \varphi_2, r_{ji}, d)$  is calculated and used in the following data transmission.

When the transmission of the real data starts, both of the LEDs operate to transmit the encoded signals simultaneously. The Align Phase button on the signal generator is pressed to ensure that the two signals are transmitted synchronously in the whole real data communication period.

## 5 Experimental Results and Analysis

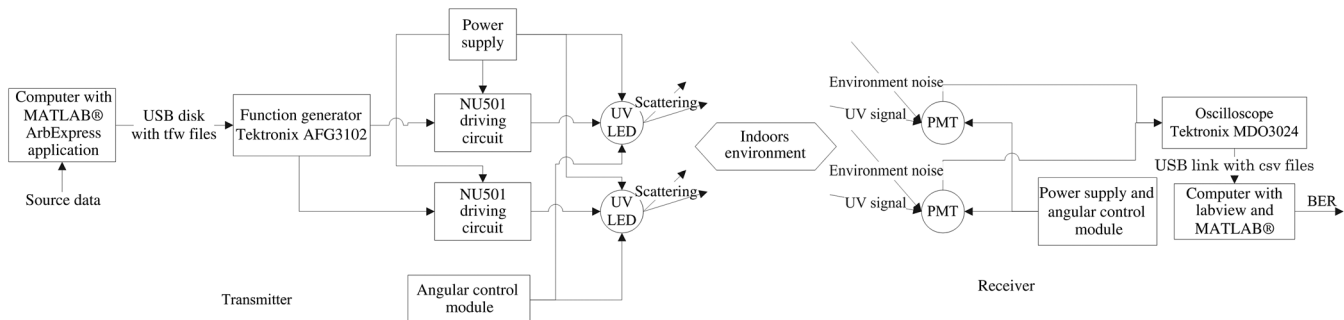
### 5.1 Experiment 1: Bit Error Rate Performance Versus Distance with Single-Input Single-Output, 1 × 2 Maximal Ratio Combining, Modified 2 × 1 Alamouti Code, and Modified 2 × 2 Alamouti Code

Figure 7 shows the BER performances of SISO, 1 × 2 MRC, modified 2 × 1 Alamouti code, and modified 2 × 2 Alamouti code versus distance in the experiments. The result shows that the 2 × 2 Alamouti code has a great advantage over the others regarding the BER performance. 1 × 2 MRC performs better than 2 × 1 Alamouti code when the distance is < 4 m, and a little worse when the distance ranges from 4 to

9 m. When the distance becomes > 9 m, the two algorithms turn to be almost the same. SISO performs the worst of all. The trend of BER versus distance of the four algorithms in the experiment is similar to those of the simulation results, which can be illustrated by the diversity gain. 2 × 1 Alamouti code and 1 × 2 MRC have the same diversity gain, which is less than that of 2 × 2 Alamouti code. SISO has no diversity gain. We also notice that the BER of the experiment result is much larger than that in the simulation result, and the transmission distance is much shorter.

### 5.2 Experiment 2: Bit Error Rate Performance Versus Transmitter Elevation and Receiver Elevation with the Modified 2 × 1 Alamouti Code and the Modified 2 × 2 Alamouti Code

Experiment 2 was performed to compare the modified 2 × 1 Alamouti code and the modified 2 × 2 Alamouti code more deeply. Figure 8 shows the BER performance of the Alamouti code versus the Tx elevation angle, and Fig. 9 shows the BER performance of the Alamouti code versus the Rx elevation angle. As the results show, 2 × 2 Alamouti code outperforms 2 × 1 Alamouti code. Notice that when the Tx elevation angle varies, 2 × 2 Alamouti code is much more instable than 2 × 1 Alamouti code, which is quite different from the simulation results. As the Alamouti code needs CSI to decode, 2 × 2 Alamouti code needs more information than 2 × 1 Alamouti code. The inaccuracy of the measure of CSI will cause more error in 2 × 2 Alamouti code. In Figs. 8 and 9, the BER of 2 × 1 Alamouti code and 2 × 2 Alamouti code mostly



**Fig. 6** Implementation of the offline experiment.

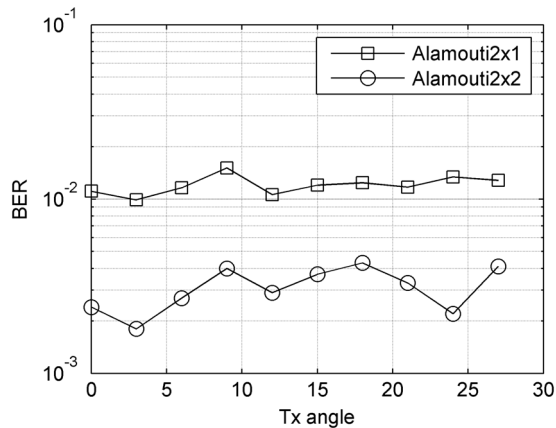


**Fig. 8** BER performance of the Alamouti codes versus distance, with Rx elevation of 10 deg and distance of 6 m.

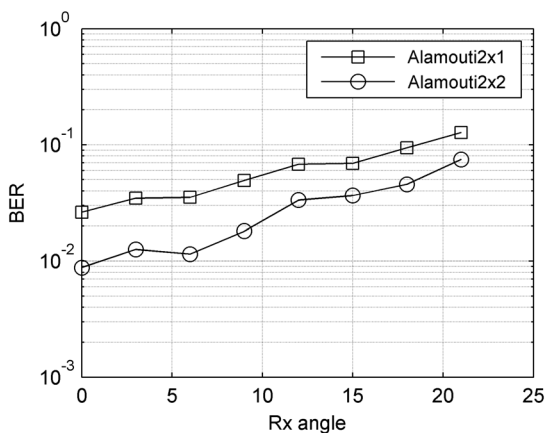


**Fig. 9** BER performance of the Alamouti codes versus distance, with Tx elevation of 10 deg and distance of 6 m.

grow slightly. Here is some analysis of this phenomenon. In normal UV communication, the receivers receive UV light from the transmitters through the atmosphere scattering. Owing to the cold weather, our experiments were carried indoors and the distance between the transmitters (or receivers) and the ceiling is  $\sim 3$  m. Because of this, there would be some strong light reflection in the experiment in addition to the atmosphere scattering. When the Rx elevation is fixed at 10 deg and the Tx elevation angle increases, the fixed receiver can always receive the UV light well because of the reflection from the ceiling and the atmosphere scattering. So the BER of each curve in Fig. 8 is almost the same. Meantime, when the Tx elevation is fixed at 10 deg and the Rx elevation angle grows, the receivers cannot always receive the UV light well especially when the Rx elevation grows to 12 deg or more. So in Fig. 9, when the Rx elevation grows from 0 to 9 deg, the BER value grows slightly. And the BER becomes bigger when the Rx elevation grows to 12 deg or more. Besides, the BER value of experimental result is worse than that of the simulation result.

### 5.3 Thoughts and Analysis of the Experimental Results and Simulation Results

As shown above, the BER of the experimental results is much larger than that in the simulation results. Many factors

underlay. In our opinion, the most important reason for the results is that the CSI earned in the experiment is not accurate. As shown in Sec. 3, the CSI is extremely important for the Alamouti code. Inaccuracy of the CSI estimation will lead to calculation error when decoded, which will obviously increase the number of error bits. In our experiment, for the efficiency of the data transmission, we only acquired the UV CSI at the beginning of the communication, which is used in the whole data communication period. And the UV MIMO CSI is time varying, which leads to imperfection in the CSI used in the receivers. Thus, the obtainment and estimation of the CSI is a critical job in the Alamouti code scheme for the whole information transmission.

## 6 Conclusion

The Alamouti code utilizes the transmitting signal orthogonally and obtains the diversity gain with the use of a simple decoding scheme. The modified Alamouti code is used in the UV MIMO communication system to adopt the UV communication character and obtain the diversity gain. As a result of our simulation and offline experiment, we conclude that a lower system BER can be achieved compared with that of the SISO or SIMO system. The numerical results from the MATLAB<sup>®</sup> simulation and the offline experiment were analyzed. As Alamouti code scheme takes CSI as an essential part, which is difficult to obtain and maintain in the real application cases, the application of the Alamouti code and even other MIMO schemes with the need of perfect CSI is limited. Study of the other STC without the need of channel information for the UV communication system is important and necessary.

## Acknowledgments

This work was supported by the National Natural Science Foundation of China (Grant Nos. 61271178 and 61471052) and the Research Innovation Fund for College Students of Beijing University of Posts and Telecommunications.

## References

1. G. Bauch and A. Alexiou, "MIMO technologies for the wireless future," in *IEEE 19th Int. Symp. on Personal, Indoor and Mobile Radio Communications*, pp. 1–6 (2008).
2. S. K. Jayaweera and H. V. Poor, "Capacity of multiple-antenna systems with both receiver and transmitter channel state information," *IEEE Trans. Inf. Theory* **49**(10), 2697–2709 (2003).
3. J. Tao, J. Wu, and Y. R. Zheng, "Reliability-based turbo detection," *IEEE Trans. Wireless Commun.* **10**(7), 2352–2361 (2011).
4. D. Gesbert et al., "From theory to practice: an overview of MIMO space-time coded wireless systems," *IEEE J. Sel. Areas Commun.* **21**(3), 281–302 (2003).
5. S. M. Alamouti, "A simple transmit diversity technique for wireless communications," *IEEE J. Sel. Areas Commun.* **16**(8), 1451–1458 (1998).
6. M. Noshad, M. Brandt-Pearce, and S. G. Wilson, "NLOS UV communications using M-ary spectral-amplitude-coding," *IEEE Trans. Commun.* **61**(4), 1544–1553 (2013).
7. A. A. Jaime, A. N. Mark, and V. V. Bane, "Multi-beam space-time coded systems for optical atmospheric channels," *Proc. SPIE* **6304**, 63041B (2006).
8. M. Niu, J. Cheng, and J. F. Holzman, "Alamouti-type STBC for atmospheric optical communication using coherent detection," *IEEE Photonics J.* **6**(1), 7900217 (2014).
9. S. G. Wilson et al., "Optical MIMO transmission using Q-ary PPM for atmospheric channel," in *Conf. Record of the Thirty-Seventh Asilomar Conf. on Signals, Systems and Computers*, Vol. 1, pp. 1090–1094 (2003).
10. X. Ke, L. Yuan, and F. Li, "Research progress of space-time code in wireless optical communications (II)," *Infrared Laser Eng.* **42**(8), 2137–2145 (2013).

11. X. Ke, J. Zhan, and Z. Li, "Research progress of space-time code in wireless optical communications (III)," *Infrared Laser Eng.* **42**(9), 2496–2504 (2013).
12. A. Gupta and M. Brandt-Pearce, "Receiver design for shot noise limited MIMO FSO/UV communication systems," in *IEEE Globecom Workshops*, pp. 1183–1187 (2012).
13. E. Bayaki and R. Schober, "On space-time coding for free-space optical systems," *IEEE Trans. Commun.* **58**(1), 58–62 (2010).
14. M. K. Simon and V. A. Vlnrotter, "Alamouti-type space-time coding for free-space optical communication with direct detection," *IEEE Trans. Wireless Commun.* **4**(1), 35–39 (2005).
15. D. Han et al., "Research on multiple-scattering channel with Monte Carlo model in UV atmosphere communication," *J. Opt. Soc. Am.* **52**(22), 5516–5522 (2013).
16. D. M. Reilly and C. Warde, "Temporal characteristics of single-scatter radiation," *J. Opt. Soc. Am.* **69**, 464–470 (1979).
17. P. Luo et al., "Performance analysis of short-range NLOS UV communication system using Monte Carlo simulation based on measured channel parameters," *J. Opt. Soc. Am.* **20**, 23489–23501 (2012).
18. P. Vainikainen et al., "Experimental characterisation of MIMO propagation channels," in *Proc. of the XXVIIth General Assembly of the Int. Union of Radio Science*, pp. 17–24 (2002).

**Li Guo** is a professor in the Research Center of Information Theory and Technique, Beijing University of Posts and Telecommunications, Key Lab of Universal Wireless Communications, Ministry of Education. Her major research interests include the future communication,

mobile clouding computing, data mining based on the mobile Internet, and embedded system design.

**Kunlun Liu** is working toward his master's degree in the School of Information and Communication Engineering, Beijing University of Posts and Telecommunications, Beijing, China. His main interest is wireless communication networks.

**Dedan Meng** is working toward her master's degree in the School of Information and Communication Engineering, Beijing University of Posts and Telecommunications, Beijing, China. Her main interest is wireless communication networks.

**Xidong Mu** is working toward his master's degree in the School of Information and Communication Engineering, Beijing University of Posts and Telecommunications, Beijing, China. His main interest is wireless communication networks.

**Dahai Han** received his PhD degree in 2007 from Beijing University of Posts and Telecommunications, Beijing, China, and he was promoted to assistant professor in 2012. His research interests include all optical transmission network and wireless optical communication. His engineering applications include internet of things and sensor network and practical application of wireless optical industry.